General Disclaimer

One or more of the Following Statements may affect this Document

- This document has been reproduced from the best copy furnished by the organizational source. It is being released in the interest of making available as much information as possible.

- This document may contain data, which exceeds the sheet parameters. It was furnished in this condition by the organizational source and is the best copy available.

- This document may contain tone-on-tone or color graphs, charts and/or pictures, which have been reproduced in black and white.

- This document is paginated as submitted by the original source.

- Portions of this document are not fully legible due to the historical nature of some of the material. However, it is the best reproduction available from the original submission.

X-621-71-202
PREPRINT

PROBE AND RADAR ELECTRON TEMPERATURES IN AN ISOTROPIC, NON-EQUILIBRIUM PLASMA

W. R. HOEGY

APRIL 1971

GSFC — GODDARD SPACE FLIGHT CENTER —
GREENBELT, MARYLAND

X-621-71-202

PROBE AND RADAR ELECTRON TEMPERATURES IN AN ISOTROPIC, NON-EQUILIBRIUM PLASMA

W. R. Hoegy

Laboratory for Planetary Atmospheres

April 1971

GODDARD SPACE FLIGHT CENTER
Greenbelt, Maryland 20771

PROBE AND RADAR ELECTRON TEMPERATURES IN AN ISOTROPIC, NON-EQUILIBRIUM PLASMA

W. R. Hoegy
Laboratory for Planetary Atmospheres

ABSTRACT

Electron temperatures measured by electrostatic probes and radar backscatter are distinct physical quantities with the temperature from each technique determined from a different moment of the electron distribution function. Numerical inequality of temperatures results from a non-Maxwellian electron distribution function or equivalently, a non-equilibrium electron plasma. Probe and backscatter electron temperatures are studied for low and high energy (isotropic) distortions of the distribution function. The non-equilibrium plasma generally produces higher probe than backscatter temperatures, however the temperature difference is small for distortions due to realistic photoelectron fluxes. If large temperature differences occur in the ionosphere, both probe and backscatter temperatures would differ from the temperature characterizing the average electron kinetic energy, and a single temperature applicable to a variety of physical processes would no longer exist.

CONTENTS

INTRODUCTION

Comparisons of electron temperatures reduced from electrostatic probe and radar backscatter measurements have resulted in a temperature discrepancy, with higher probe than backscatter temperatures [Hanson et al, 1969; Carlson and Sayers, 1970; Booker and Smith, 1970; Brace and McClure, 1971]. Some comparisons have demonstrated agreement among the probe and backscatter temperatures [Brace, et al, 1969; Taylor and Wrenn, 1970]. Two possible explanations for the discrepancy have been suggested recently: the presence of suprathermal electrons in the electron distribution function (Waldteufel, 1969) and the slow variation of the contact potential of the probe surface (Carlson and Sayers, 1970). The contact potential variation in laboratory probes has been eliminated by probe heating and by a rapid sweep of the probe potential [Waymouth, 1959]. However it has not been firmly established that rocket and satellite probe electron temperatures are significantly affected by the contact potential variation. Several authors have discussed this and other possible sources of error in the probe temperature measurements and have in general confirmed the technique [Wilmore, 1970; Brace et al., 1970].

As regards the effect on the probe and radar temperatures due to an enhanced energetic electron population, only the effect on the radar temperatures has been discussed in the literature.

We investigate the effect of an isotropic non-Maxwellian electron distribution function on both probe and radar electron temperatures. This distribution represents a simplification of actual ionospheric conditions, nevertheless it allows us to study the important case of energetic photoelectrons as well as to illustrate the basic theoretical difference in the temperature parameters of the two techniques.

DISTRIBUTION FUNCTION

The isotropic electron distribution, f(v), is used in two representations: 1) as a sum of two Maxwell distributions at temperatures T_1 and T_2 and with populations 1-p and p respectively,

$$f(v) = (1 - p)\left(\frac{m}{2\pi k T_1}\right)^{3/2} e^{-mv^2/2kT_1} + p\left(\frac{m}{2\pi k T_2}\right)^{3/2} e^{-mv^2/2kT_2} \qquad (1)$$

and 2) as a Laguerre polynomial expansion

$$f(v) = \left(\frac{m}{2\pi k T}\right)^{3/2} e^{-mv^2/2hT} \sum_{\ell=0}^{\infty} A_\ell L_\ell^{(1/2)}\left(\frac{m v^2}{2 k T}\right) \qquad (2)$$

$$A_0 = 1,\ A_1 = 0$$

The two-temperature distribution, Eq. 1, may be used to represent the presence of energetic photoelectrons when $T_2 > T_1$, and $P << 1$, and a distorted low energy electron population for nearly equal values of T_1 and T_2. The coefficients A2, A3, etc. in the polynomial representation determine the deviation from a Maxwell distribution. When $T_2/T_1 < 10$, then the two temperature distribution can be represented by the Laguerre polynomial expansion, however the latter can represent a greater variety of non-equilibrium situations.

TEMPERATURE DEFINITIONS

The probe and radar temperature parameters are determined from different moments of the electron distribution function. Each temperature is therefore a distinct physical parameter since it samples a different portion of the electron

energy spectrum. There is strict numerical equality of the temperatures only when the distribution function is pure Maxwellian. Historically the probe and radar temperatures have been considered identical physical parameters since the assumption of a Maxwell distribution has been inherent in the theories of the two techniques. We shall examine the extent of the probe and radar temperature difference for an assumed deviation from a Maxwell distribution, or degree of departure of the ionosphere from equilibrium. In the following we review the definitions of four instrument temperatures (three probes and one radar) and the thermodynamic temperature, which definitions are valid for any isotropic distribution function (with unit normalization).

The thermodynamic temperature, T_{th}, is determined from the average energy of the entire electron population,

$$3/2\ k\ T_{th} = \int d\ v\ \frac{1}{2}\ m\ v^2\ f\ (v). \tag{3}$$

The radar backscatter electron temperature, T_b, is one of several parameters determining the shape of the backscatter power spectrum [Rosenbluth and Rostoker, 1962]. The ion component of the power spectrum, neglecting terms of order $(m_e/m_i)^{1/2}$, depends on the electron distribution function only through the integral,

$$\frac{m}{k\ T_b} = \int d\ v\ \frac{1}{v^2}\ f\ (v). \tag{4}$$

Thus the effect of a distorted isotropic electron distribution function on the radar electron temperature can be studied without analyzing the power spectrum or the correlation function. The velocity moment defining T_b gives more weight to the low energy electrons than the moment defining T_{th}.

The three probe temperatures are defined in terms of the retarded electron current

$$i = K \int_{\sqrt{2eV/m}}^{\infty} v\, dv \left(v^2 - \frac{2eV}{m}\right) f(v). \tag{5}$$

where K is a constant depending on the probe geometry and V is the absolute magnitude of potential difference between the probe and plasma. The probe temperature, T_{plate}, corresponds to the temperature measured by the a.c. mode Langmuir plate [Wrenn, 1969]. This device, by operating in the a.c. mode, measures the ratio of the first to the second derivative of the electron current. Thus T_{plate} is defined by,

$$T_{plate} = \frac{m}{k} \int_{\sqrt{2eV/m}}^{\infty} v\, dv\, f(v) / f\left(\sqrt{\frac{2eV}{m}}\right) \tag{6}$$

The extent of the variation of T_{plate} with potential can in principle provide information on the electron distribution function, even though it does not directly measure f(v).

The temperature, T_{cyl}, corresponds to the temperature measured by the cylindrical electrostatic probe [Findlay and Brace, 1969]. The temperature

T_{cyl} is that parameter which gives the best fit of the retarded electron current to an exponential of the potential over a given range of potentials. In order to separate the retarded current from the net current, we adopt the procedure set forth by Theis [1968]. The parameter T_{cyl} is determined from a best fit to the net current, using the four parameter expression,

$$i_{net} = C_1 e^{-eV/kT_{cyl}} + C_2 + C_3 V. \tag{7}$$

Some information on the electron distribution function can be obtained by varying the voltage interval over which the fit is made.

The temperature, T_{trap}, corresponds to the temperature measured by the planar electron trap [Donley, 1969]. This device measures the retarded electron current over a wide voltage range, enabling it to detect both the thermal and the energetic electrons. We define T_{trap} from the slope of ln i versus V,

$$T_{trap} = \frac{m}{2k} \int_{\sqrt{2eV/m}}^{\infty} v\, dv \left(v^2 - \frac{2eV}{m}\right) f(v) \Big/ \int_{\sqrt{2eV/m}}^{\infty} v\, dv\, f(v) \tag{8}$$

We now specialize the five temperature definitions for the case of the two-temperature distribution function. The thermodynamic and backscatter temperatures have a simple form,

$$T_{th} = (1 - p)\, T_1 + p\, T_2 \tag{9}$$

$$1/T_b = (1 - p)/T_1 + p/T_2. \tag{10}$$

As a consequence of these definitions, $T_{th} \geq T_b$ with equality holding when p = 0, 1, and with the greatest difference occuring when p = 1/2. The retarded electron current reduces to the sum of two exponentials,

$$(1 - p)\ \sqrt{T_1}\ e^{-eV/kT_1} + p\sqrt{T_2}\ e^{-eV/kT_2}, \tag{11}$$

thus the trap and plate temperatures are given by,

$$T_{trap} = (1 - q)\ T_1 + q\ T_2, \tag{12}$$

$$1/T_{plate} = (1 - q)/T_1 + q/T_2, \tag{13}$$

$$q = \frac{p/\sqrt{T_2}\ e^{-eV/kT_2}}{\frac{1 - p}{\sqrt{T_1}}\ e^{-eV/kT_1} + p/\sqrt{T_2}\ e^{-eV/kT_2}} \tag{14}$$

It follows from Eqs. 12-14 that for a two-temperature distribution, $T_{trap} \geq T_{plate}$, with equality holding for p = 0, 1. (This inequality holds only if both measurements are taken at the same voltage.) The parameter, T_{cyl} is given by fitting the current of Eq. 7 to the form of Eq. 11.

Next we specialize the temperature definitions for the Laguerre polynomial expanded distribution function. The thermodynamic and backscatter temperatures are,

$$T_{th} = T, \tag{15}$$

$$T_b = T / \sum_{\ell=0}^{\infty} A_\ell . \tag{16}$$

There is no inequality relating T_{th} and T_b and either temperature could be larger than the other. The retarded electron current, used to define the probe temperatures, is given as,

$$\sqrt{T}\, e^{-eV/kT} \sum_{\ell=0}^{\infty} A_\ell L_\ell^{(-3/2)} \left(\frac{e\,V}{k\,T}\right) \tag{17}$$

The temperature T_{cyl} is obtained from the four parameter fit to this current expression, and the trap and plate temperatures are

$$T_{trap} = T \frac{\sum_{\ell=0}^{\infty} A_\ell L_\ell^{(-3/2)} \left(\frac{e\,V}{k\,T}\right)}{\sum_{\ell=0}^{\infty} A_\ell L_\ell^{(-1/2)} \left(\frac{e\,V}{k\,T}\right)} \tag{18}$$

$$T_{plate} = T \frac{\sum_{\ell=0}^{\infty} A_\ell L_\ell^{(-1/2)} \left(\frac{e\,V}{k\,T}\right)}{\sum_{\ell=0}^{\infty} A_\ell L_\ell^{(1/2)} \left(\frac{e\,V}{k\,T}\right)} \tag{19}$$

We have illustrated the formal difference between the five temperature parameters, T_{th}, T_b, T_{plate}, T_{cyl}, and T_{trap}; in following sections we shall present examples of numerical temperature differences for given distortions of the distribution function from a Maxwell distribution. And in order to connect

the distortion of the distribution function with the degree of departure of the ionospheric electrons from equilibrium we shall include an evaluation of the degree of departure parameter, L, [Lunc, 1963]. The parameter L is defined by,

$$L^2 + 1 = \int d\,v\, f^2/feq, \tag{20}$$

where f_{eq} is the equilibrium distribution function. The state of the electrons is considered far from equilibrium when $L >> 1$, close to equilibrium when $L << 1$, and in a transition regime when $L \sim 1$.

The voltages used in computing the probe temperatures are: .5 volts for T_{plate}; .1 volts for T_{trap} ; .5 to 2.5 volts for T_{cyl}.

PHOTOELECTRONS

The effect on the five temperature parameters of energetic photoelectrons is examined with the two-temperature distribution function. The superthermal electrons are represented by a Maxwell distribution at temperature T_2 and with relative density p, $p << 1$, $T_2 > T_1$, where T_1 is the temperature of the low energy or thermal electrons. A convenient description of the photoelectrons is to specify their temperature, T_2, and normalized flux, Photo,

$$\text{Photo} = p\sqrt{T_2}. \tag{21}$$

(The flux is given by, $n\sqrt{k/2\pi m}$ Photo.)

The range of values of T_2 and Photo which characterize the ionospheric photoelectrons are estimated from three sources. In the first, Dalgarno McElroy and Stewart computed values of the equilibrium photoelectron flux [Dalgarno et al., 1969]. A Maxwellian fit to their 350 km flux values yields the values, $T_2 \approx 70{,}000°K$ and Photo $\approx 10^4/n$, where n is the total electron number density in part. cm^{-3}. The electron trap data of Donley at 1410 km yield the approximate values $T_2 \approx 90{,}000°K$ and Photo $\approx .8$ [Donley, 1969]. And finally Huang has made rocket measurements of superthermal electrons in the altitude range from 120 km to 240 km [Huang, 1969]. The low altitude values are approximately, $T_2 \approx$ 10,000°K to 30,000°K and Photo $\approx .3$ to .5.

The above values suggest that the ionospheric photoelectrons are characterized by the range of values,

$$T_2 = 10{,}000\,°K - 100{,}000\,°K$$

$$\text{Photo} = .1 - 1$$

The three sources are displayed as shaded areas in Figure 1 bounded by these ranges. The differences among the temperature parameters are displayed in Figures 2-5 using the same coordinates as in Figure 1 so that they may be correlated with the photoelectron regions.

The radar backscatter temperature, T_b, differs from the thermal electron temperature, T_1, by no more than 1% over the region of Figure 1, therefore for photoelectrons

$$T_b \simeq T_1.$$

In Figures 2-5 are displayed contours of the relative differences between the temperatures T_{th}, T_{plate}, T_{trap}, and T_{cyl} respectively with the thermal population temperature $T_1 = 1500°K$. The relative differences decrease as T_1 increases (or as the electrons approach equilibrium). Figure 2 shows that the temperature difference between T_{th} and T_1 is greater than 5% for Photo > .5, but that it does not exceed 20% over the entire range. The temperature difference between T_{plate} and T_1 in Figure 3 does not exceed 3% for the three regions of Figure 1. The difference between T_{trap} and T_1 remains less than 5%. In some regions the inequality, $T_{trap} \geq T_{plate}$, is violated because the voltages at which the temperatures are defined were chosen to reflect the conditions of the experiments. The difference between T_{cyl} and T_1 in Figure 5 varies between 5% and 10% in the low altitude region and is less than 3% in the higher altitude regions.

Figure 6 illustrates the variation of the five temperatures with the photoelectron energy for a fixed flux, Photo = 1, and for $T_1 = 1500°K$.

We conclude that photoelectrons produce no significant temperature differences among the four instrument temperatures, T_b, T_{trap}, T_{plate}, and T_{cyl}. An evaluation of the parameter L, Eq. 20, specifying the degree of departure of the electron gas from equilibrium shows that the electrons are far from equilibrium. (To obtain a finite value of L it is necessary to introduce a cutoff energy E above which there are no photoelectrons, a typical calculation yields $L = 3 \times 10^6$ for $T_1 = 1500°K$, $T_2 = 30{,}000°K$, Photo = .5, and E = 10 ev.) Thus the highly non-equilibrium state of the ionosphere as produced by photoelectrons, although it causes such phenomena as dayglow, yet it does not affect the probe and radar temperature measurements; they essentially measure only the thermal electron population.

The neglect of anisotropy in the photoelectron velocity distribution would not alter this conclusion. A particle precipitation producing energetic electrons at fluxes substantially higher than the fluxes of Figure 1 would produce elevated probe and radar temperatures as well as temperature differences among the five temperature parameters. Large increases in the cylinder probe temperature have been observed in coincidence with soft electron flux precipitating in the auroral region [Brace and Findlay, 1970].

DISTORTED THERMAL ELECTRONS

The effect of a distorted thermal (low energy) electron population on the probe and radar temperature parameters is first evaluated using the two-temperature distribution function. We choose the values $T_1 = 1000$, $P = .5$ (to maximize the distortion) and the range of values $T_2/T_1 = 1$ to 2. The resulting temperatures are displayed in Fig. 7. For the range of parameters shown, the three probe temperatures are greater than T_{th}, while the radar temperature is smaller than T_{th}. Therefore whenever there is a significant probe – radar temperature difference, then both instrument temperatures differ appreciably from the thermodynamic temperature.

The measure of the degree of deviation from equilibrium, L, varies from $L = .0031, .011, .023$ at $T_2/T_1 = 1.1, 1.2, 1.3$ to $L = .133, .153$ at $T_2/T_1 = 1.9, 2.0$ respectively, thus we classify the two-temperature distribution used in Fig. 7 as lying in the transition regime or moderately close to equilibrium. This demonstrates that moderate to large temperature differences do not necessarily require the ionosphere electrons to be far from equilibrium.

Finally we examine the effect of a distorted thermal population represented by a Laguerre polynomial expansion. The first two coefficients are $A_0 = 1$, $A_1 = 0$ with the result that $T_{th} = T$, and A_2 lies in the range from 0 to .5. The five temperatures are shown in Fig. 8 for T = 1000°K. A large temperature difference results for values, $A_2 > 0.1$. Again the three probe temperatures lie above T_{th} while the radar temperature lies below.

An examination of the distribution function in Fig. 9 shows that the slope becomes steeper as A_2 increases at low energies with the opposite behavior at high energies. A steeper slope results in a smaller temperature. Therefore since the radar backscatter samples only the low energy electrons, it gives a lower temperature as A_2 increases while the probes sample the higher energy electrons and consequently give a higher temperature as A_2 increases.

The parameter, L, giving the degree of deviation from equilibrium ranges from L = .137 for $A_2 = .1$ to L = .685 for $A_2 = .5$. Figure 10 shows the variation of the relative probe to radar temperature difference versus the extent of deviation from equilibrium for the distorted thermal electron population. The points from the two-temperature distribution and the polynomial expanded distribution tend to follow the same curve. From the curves we see that for example a 50% temperature difference corresponds to L values of approximately .15 to .34.

It must be noted that in contrast with the photoelectron distribution function we do not have realistic values for the parameters of the distorted thermal distribution functions that would typify the ionosphere. Therefore rather than

setting limits on what temperature differences can exist in the ionosphere due to a known, distortion of the low energy electron distribution we have demonstrated what distortion is necessary to produce a given temperature difference.

SUMMARY

An examination of the probe and radar electron temperatures for an isotropic non-Maxwellian electron distribution function has demonstrated the distinctiveness of each probe and radar temperature parameter, in both the energies and the methods of sampling the electrons. We find that a realistic photoelection population does not produce significant temperature differences. Large temperature differences, 50% or more, can result from higher than normal fluxes of energetic electrons or from a distorted low energy electron population. If the electron distribution function can be characterized by a different temperature above and below about 1KT as illustrated in Fig. 9 then the probe and radar temperatures will be quite different since they sample in the higher and lower energy regions respectively. In the development and use of the probe and radar techniques, the Maxwellian form of the distribution function has been a basic assumption. Consequently neither technique has been operated in a manner allowing it to measure the electron distribution function at low energies. It is hoped that future investigations, both experimental and theoretical, will study the ionospheric electron distribution function, particularly in the energy range below 2 ev. Such studies will be of great interest not only for the temperature discrepancy problem but also for understanding the myriad of ionosphere electron interactions.

If the isotropic ionospheric electron distribution function were sufficiently distorted from a Maxwellian form to produce large probe – backscatter temperature differences as illustrated in the sample calculations, then one would not be

justified in using a single temperature parameter in all calculations of physical quantities (such as energy, thermal conductivity, etc.) nor would one be able to assign a preference for one instrument temperature over another. The probe and backscatter measurements would in this case provide complimentary information. However the relevant parameter to be measured would then be the electron distribution function itself.

ACKNOWLEDGMENTS

The author would like to thank Dr. H. G. Mayr, Mr. L. H. Brace, and Prof. A. P. Willmore for some stimulating discussions. The computations were performed in APL on the IBM 360/95.

REFERENCES

1. Booker, H. G. and E. K. Smith, A Comparative Study of Ionospheric Measurement Techniques, J. Atm. Terr. Phys., 32, 467, 1970.
2. Brace, L. H., and J. A. Findlay, ISIS-1 Electron Temperature Observation in the Auroral Zone, paper presented at annual AGU meeting, April 1970, Washington, D. C., 1970.
3. Brace, L. H. and J. P. McClure, Comparisons of Equatorial Rocket Probe and Radar Observations, paper presented at AGU annual meeting, Washington, D. C., 1971.
4. Brace, L. H., H. C. Carlson, and K. K. Mahajan, Radar Backscatter and Rocket Probe Measurements of Electron Temperature above Arecibo, J. Geophys, Res., 74, 1883, 1969.
5. Brace, L. H., G. R. Carignan, and J. A. Findlay, Experiental Evaluation of Ionosphere Electron Temperature Measurements by Cylindrical Electrostatic Probes, XIII th Plenary meeting, COSPAR, Leningrad, 1970.
6. Carlson, H. C. and J. Sayers, Discrepancy in Electron Temperatures Deduced from Langmuir Probes and from Incoherent Scatter Radars, J. Geophys. Res., 75, 4883, 1970.
7. Dalgarno, A., M. B. McElroy, and A. I. Stewart, Electron Impact Excitation of the Dayglow, J. Atm. Sci., 26, 753, 1969.
8. Donley, J. L., The Thermal Ion and Electron Trap Experiments on the Explorer XXXI Satellite, Proc. IEEE, 57, 1061, 1969.

9. Findlay, J. A., and L. H. Brace, Cylindrical Electrostatic Probes Employed on Alouette II and Explorer XXXI Satellites, Proc. IEEE, 57, 1054, 1969.

10. Hanson, W. B., L. H. Brace, P. L. Dyson, and J. P. McClure, Conflicting Electron Temperature Measurements in the Upper F Region, J. Geophys. Res. 74, 400, 1969.

11. Huang, P. T., Direct Measurements of Electron Energy Distributions in the Daytime Ionosphere, Ph. D. thesis, U. of Maryland 1969, Maryland Tech. report 936, 1969.

12. Lunc, M., A Criterion for the Degree of Departure from Equilibrium and its Application to Rarefield Gases, Proc. Intern. Symp. Rarefield Gas Dyn. 3rd, Paris 1962, Vol I, 94, 1963.

13. Rosenbluth, M. N., and N. Rostoker, Scattering of Electromagnetic Waves by a Nonequilibrium Plasma, Phys. of Fluids, 5, 776, 1962.

14. Taylor, G. N. and G. L. Wrenn, Comparisons of Simultaneous Satellite and Ground-based Measurements of Ionospheric Parameters, Planet and Space Sci., 18, 1663, 1970.

15. Theis, R. F., Computer Derivation of Geophysical Data from Satellite Electrostatic Probe Measurements, NASA-GFSC Tech. Note, X621-68-481, 1968.

16. Waldteufel, P., Influence Sur Les Measures Ionosphériques Par Diffusion de Thomson d'une Distribution Électronique non Maxwellienne, Ann. Géophys., 25, 381, 1969.

17. Waymouth, J. R., Pulse Technique for Probe Measurements in Gas Discharges, J. Appl. Phys., 30, 1404, 1959.

18. Wilmore, A. P., Electron and Ion Temperatures in the Ionosphere, NASA-GFSC Tech. Note X621-70-145, 1970.

19. Wrenn, G. L., The Langmuir Plate and Spherical Ion Probe Experiments Aboard Explorer XXXI, Proc. IEEE, 57, 1072, 1969.

LIST OF FIGURES

Figure 10. Relative temperature difference between probe and radar correlated with the extent of deviation of electrons from equilibrium. Solid curves computed with polynomial expanded distribution, dashed curves computed with two temperature distribution.

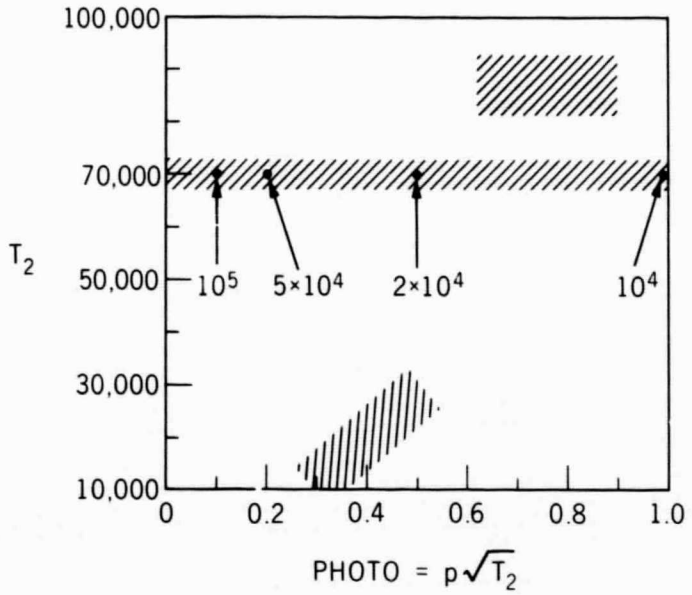

Figure 1. Photoelectron regions for various temperature and flux values. Numbers at 70,000 °K represent ambient density in particles per cc.

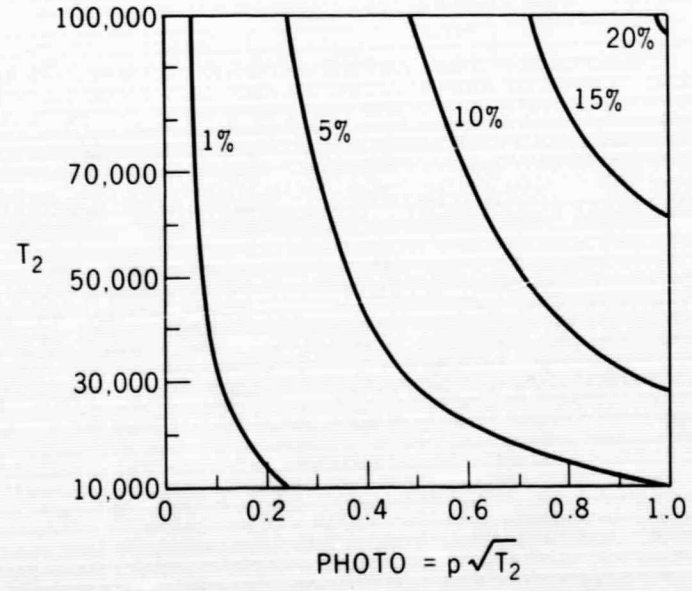

Figure 2. Contours of relative difference between thermodynamic temperature and T_1 for photoelectrons. T_1 =1500 °K.

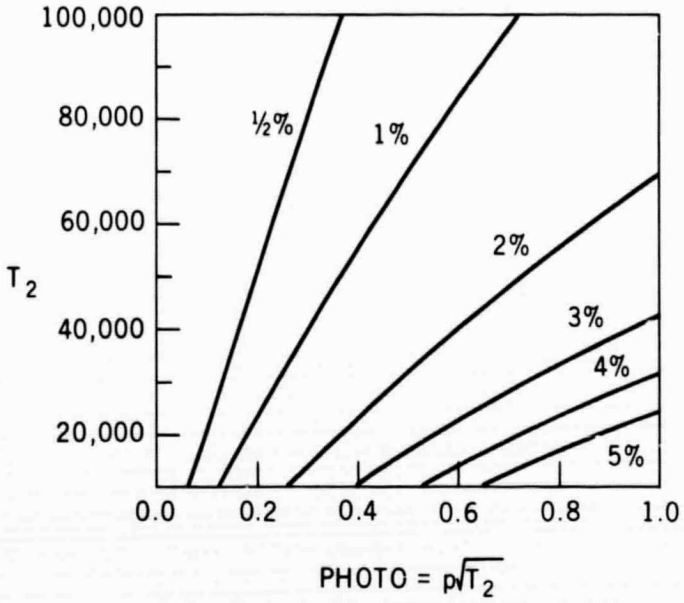

Figure 3. Contours of relative difference between a.c. plate probe temperature and T_1 for photoelectrons. T_1 =1500°K, V =.5 volts.

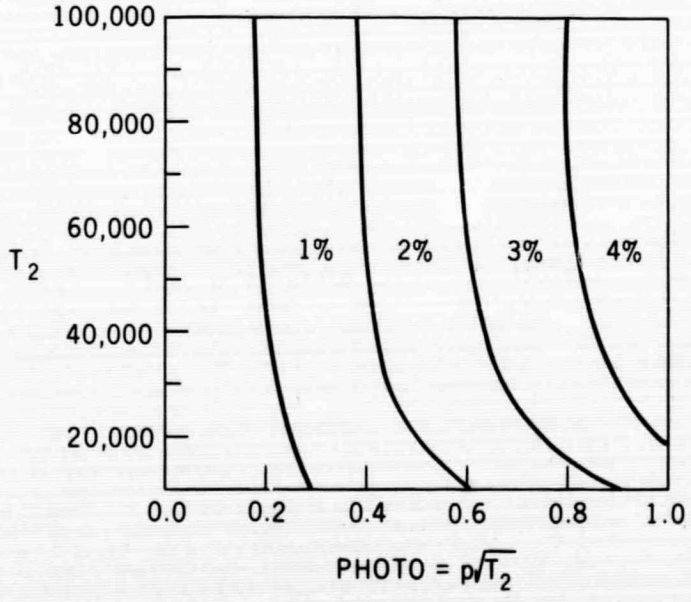

Figure 4. Contours of relative difference between electron trap temperature and T_1 for photoelectrons. T_1 =1500°K, V =.1 volt.

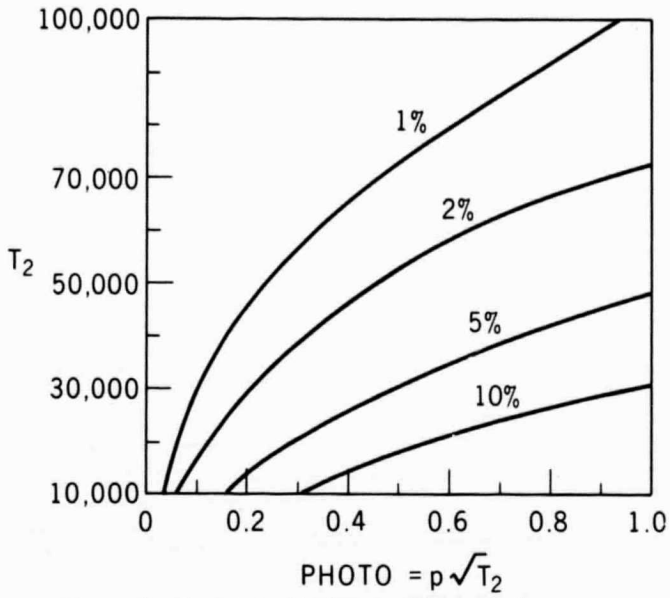

Figure 5. Contours of relative difference between cylinder probe temperature and T_1 for photoelectrons. T_1 = 1500° K, V = .5 to 2.5 volts.

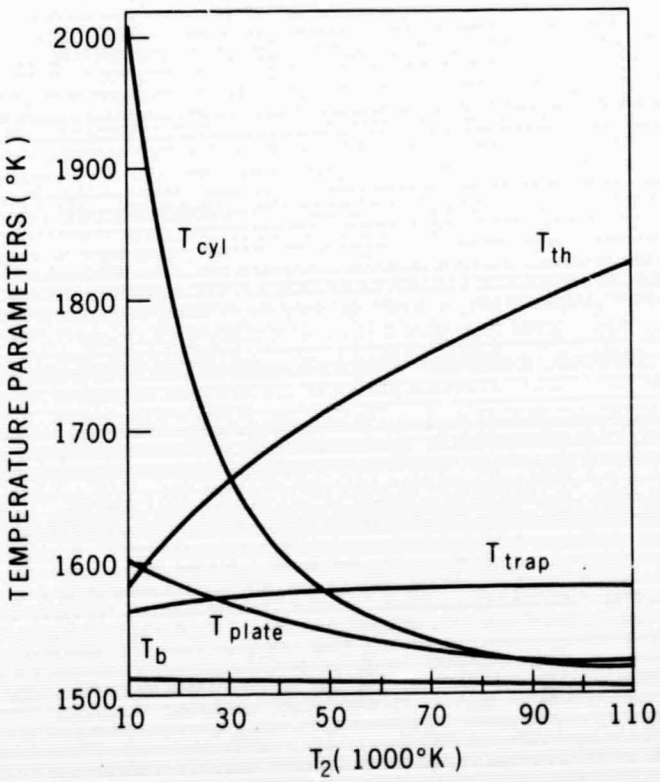

Figure 6. Variation of the five temperature parameters with photoelectron temperature. T_1 = 1500°K, Photo = 1.

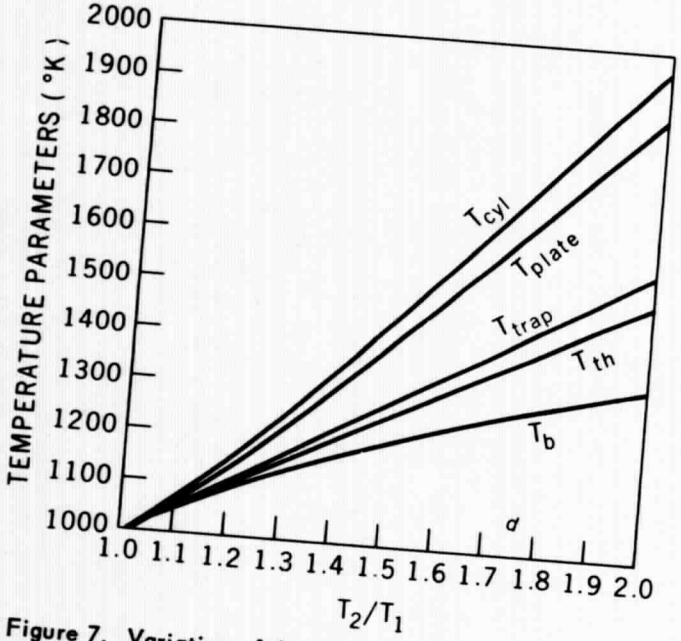

Figure 7. Variation of the five temperature parameters with temperature ratio T_2/T_1 for a two-temperature distribution function. $P = 1/2$, $T_1 = 1{,}000°K$.

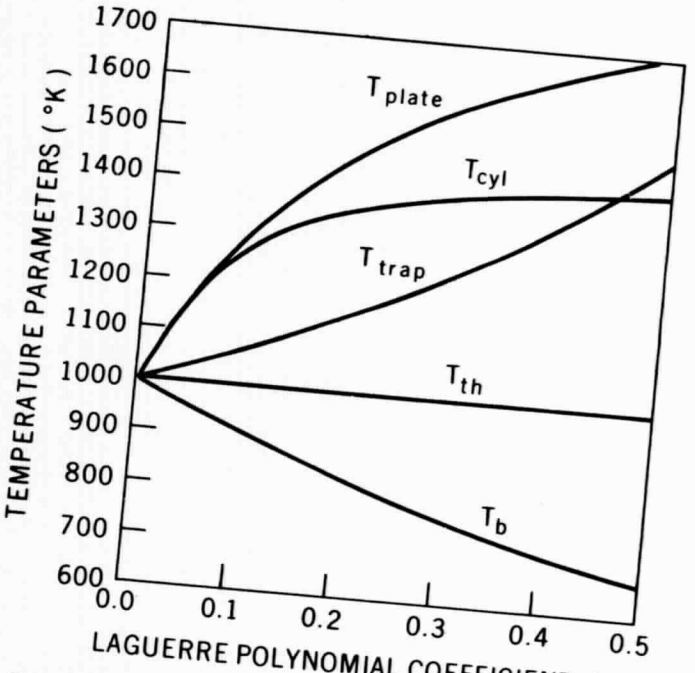

Figure 8. Variation of the five temperature parameters with the coefficient A_2 for a Laguerre polynomial expanded distribution function. $T = 1{,}000°K$.

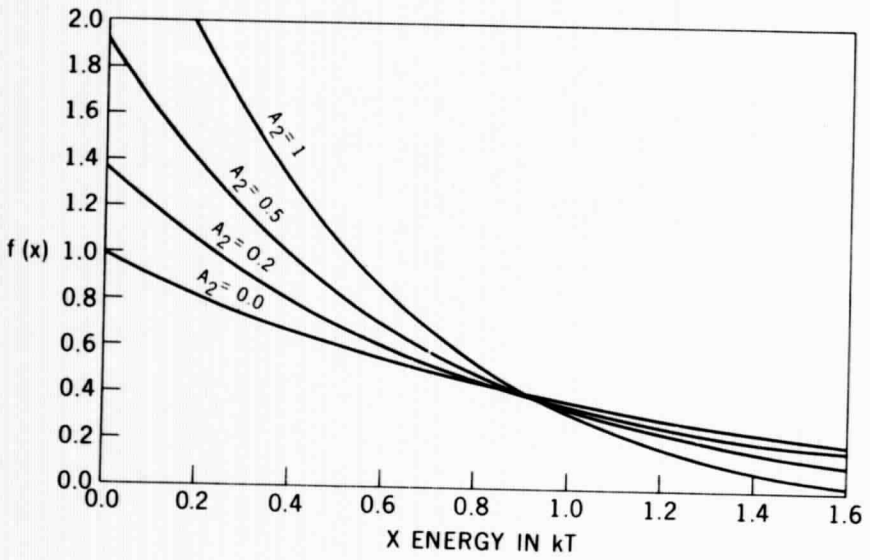

Figure 9. Laguerre polynomial expanded distribution function, $f(x) = e^{-x}\,[1 + A_2\,\{15/8 - 5/2\,x + x^2/2\}]$.

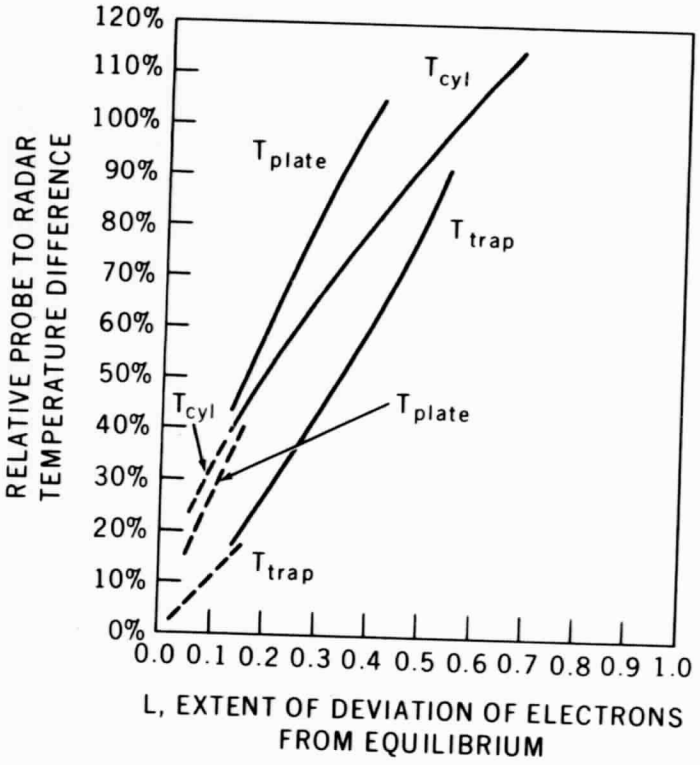

Figure 10. Relative temperature difference between probe and radar correlated with the extent of deviation of electron from equilibrium. Solid curves computed with polynomial expanded distribution, dashed curves computed with two temperature distribution.